Erratum

Engstler, M., Thilo, L., Weise, F., Grünfelder, C. G., Schwarz, H., Boshart, M. and Overath, P. (2004). Kinetics of endocytosis and recycling of the GPI-anchored variant surface glycoprotein in *Trypanosoma brucei*. *J. Cell Sci.* **117**, 1105-1115.

Equations 1 and 2 were published incorrectly in both the print and online versions of the paper. The corrected equations are shown below. We apologise for any inconvenience caused.

$$n_e^*(t)/n_s = A \times [1 - e^{-K \times (t-L)}] \times e^{-Kd \times (t-L)} \qquad (1)$$

$$n_s^*(t)/n_s = A \times e^{-Kb \times (t-L)} \times [1 - e^{-K \times (t-L)}] + [1 - e^{-Kb \times (t-L)}] \qquad (2)$$

Kinetics of endocytosis and recycling of the GPI-anchored variant surface glycoprotein in *Trypanosoma brucei*

Markus Engstler[1,*], Lutz Thilo[3], Frank Weise[2], Christoph G. Grünfelder[2], Heinz Schwarz[4], Michael Boshart[1] and Peter Overath[2,*]

[1]Ludwigs-Maximilians-Universität, Department Biologie I, Bereich Genetik, Maria-Ward-Strasse 1a, D-80638 München, Germany
[2]Max-Planck-Institut für Biologie, Abteilung Membranbiochemie, Corrensstrasse 38, D-72076 Tübingen, Germany
[3]Division of Medical Biochemistry, University Cape Town Medical School, Anzio Road, ZA-7925 Observatory, South Africa
[4]Max-Planck-Institut für Entwicklungsbiologie, Spemannstrasse 35, D-72076 Tübingen, Germany
*Authors for correspondence (e-mail: engstler@lrz.uni-muenchen.de; peter.overath@tuebingen.mpg.de)

Accepted 14 October 2003
Journal of Cell Science 117, 1105-1115 Published by The Company of Biologists 2004
doi:10.1242/jcs.00938

Summary

The dense coat of glycosylphosphatidylinositol (GPI)-anchored variant surface glycoprotein (VSG) covering parasitic African trypanosomes is essential for survival in mammalian hosts. VSG is internalised and recycled exclusively via a specialised part of the plasma membrane, the flagellar pocket. Direct measurement of the kinetics of VSG endocytosis and recycling shows that the VSG cell-surface pool is turned over within 12 minutes. Correspondingly, the turnover of the intracellular pool (9±4% of total VSG) requires only 1 minute, and this is an exceptionally high rate considering that endocytosis and exocytosis are limited to only 5% of the cell surface area. Kinetic 3D co-localisation analysis using biotinylated VSG and a panel of compartmental markers provides consistent evidence for the itinerary of VSG through the cell: VSG is endocytosed in large clathrin-coated vesicles, which bud from the flagellar pocket membrane at a rate of 6-7 vesicles per second, and is then delivered to RAB5-positive early endosomes. From there, VSG is recycled to RAB11-positive recycling endosomes at two stages, either directly or via RAB7-positive, late endosomes. Small clathrin-coated vesicles carrying fluid-phase cargo and being depleted of VSG bud from early and recycling endosomes. These vesicles are postulated to deliver their content to late endosomes and/or the lysosome. The recycling endosomes give rise to RAB11-positive exocytic carriers that fuse with the flagellar pocket and thereby return VSG to the cell surface. VSG recycling provides an interesting model for studies on the cellular trafficking and sorting of GPI-anchored proteins.

Key words: Endocytosis, Recycling, Glycosylphosphatidylinositol, Deconvolution microscopy, Quantitative colocalisation, *Trypanosoma brucei*

Introduction

Unravelling the mechanisms of endocytosis, as well as of the ensuing intracellular sorting and recycling processes, is of central importance for understanding the communication of eukaryotic cells with their environment (Mellman, 1996; Mukherjee et al., 1997; Gruenberg, 2001). For the mammalian stage of the unicellular flagellate, *Trypanosoma brucei*, which is the causative agent of sleeping sickness in man and for nagana in cattle, this environment is the mammalian vascular system that provides all the required high and low molecular weight nutrients. For several reasons, *T. brucei* provides an interesting system for studies on endo- and exocytosis, particularly in relation to the trafficking and sorting of glycosylphosphatidylinositol (GPI)-anchored proteins: First, this parasite restricts both endocytosis and exocytosis to the flagellar pocket that consists of an invagination of the plasma membrane around the emerging flagellum and comprises an area of only approximately 5% of the cell surface. Second, all endosomal membrane structures are compactly organised in the posterior half of the cell between the flagellar pocket and the nucleus. Third, each cell expresses 10^7 molecules of a predominant surface protein, the GPI-anchored variant surface glycoprotein (VSG) (Webster and Russel, 1993; Overath et al., 1997; Landfear and Ignatushchenko, 2001; Morgan et al., 2002a; Morgan et al., 2002b).

T. brucei supports fluid-phase endocytosis, which can deliver markers such as ferritin or complexes of various proteins and colloidal gold from the flagellar pocket to tubulo-cisternal endosomes and then to the perinuclear lysosome (Langreth and Balber, 1975; Webster and Grab, 1988; Frevert and Reinwald, 1988; Webster, 1989), as well as receptor-mediated endocytosis of growth factors such as transferrin and LDL (Coppens et al., 1987). VSG is conveyed to endosomes by coated vesicles and indirect evidence suggests that it is efficiently recycled (Webster and Grab, 1988; Frevert and Reinwald, 1988; Seyfang et al., 1990; Grünfelder et al., 2003). Moreover, *T. brucei* clears anti-VSG antibodies from the cell surface (Russo et al., 1993; O'Beirne et al., 1998), and this process, in addition to the well-known antigenic variation, may contribute to parasite persistence in the immuno-competent host.

The recent identification of clathrin and several marker

proteins for endosomal sub-compartments in *T. brucei* (Field et al., 1998; Morgan et al., 2001; Jeffries et al., 2001; Pal et al., 2002; Alexander et al., 2002) has provided a basis for a more detailed analysis of endocytosis and the intracellular trafficking of VSG. In the first part of this study, we quantify the rates of VSG endocytosis and recycling. In the second part, we propose an intracellular itinerary for the VSG through the endosomal compartment. We argue that this parasite has optimised endocytosis and recycling of GPI-anchored proteins as an adaptation to its unique lifestyle and therefore provides an interesting model for further analysis of this pathway.

Materials and Methods

Trypanosomes and cell culture

T. brucei MITat 1.2 expresses the wild-type (WT) VSG 221 (N-terminus of the mature protein: NH_2-AAEKGFKQAFWQPLC-) from the 221 expression site. In strain MITat 1.2-Ty-1 a *vsg 221*-gene encoding a Ty-1 tag (NH_2-AAEKG*AR***EVHTNQDP***LD*KQ-AFWQPLC-; tag in bold letters, amino acid changes because of cloning in italics) has been inserted into the 221 expression site, whereas the WT *vsg 221* gene has been deleted. Therefore, this strain synthesises the tagged VSG at WT expression levels (M.E., unpublished). The cells were grown as described before (Grünfelder et al., 2002). For MITat1.2-Ty-1, the medium contained 15 μg/ml Geneticin and 10 μg/ml Blasticidin S (ICN, Eschwege, Germany).

Antibodies

The peptide NH_2-AAEKGFKQAFWQPLC-COOH corresponding to the NH_2-terminus of VSG-221 from clone MITat 1.2 was coupled to ovalbumin via the cross-linker SPDP (Pierce, Rockford, IL) and the resulting conjugate was used to immunise rabbits or mice (nanotools Antikörpertechnik, Teningen, Germany). The resulting high-titered anti-N-terminal peptide antisera (anti-VSG-NTP) from one rabbit (H1) or one C57BL6-mouse (3-18III) was used in the VSG recycling experiments. Both antisera reacted with live MITat 1.2-Ty-1 cells but not with cells expressing WT VSG 221. Approximately 90% of the mouse serum reactivity could be abolished by acetylation of live MITat 1.2-Ty-1 cells using sulfo-NHS-acetate (Pierce). This observation provided the basis for measuring the rate of VSG recycling (see below).

Endocytosis of surface biotinylated proteins

Cultures of exponentially growing MITat 1.2 cells (5-8×10^5/ml) were divided in 50 ml tubes, chilled on ice for 10 minutes and centrifuged for 15 minutes at 750 ***g*** (1500 rpm) in a Heraeus-Christ Minifuge GL in the cold. Cells were washed twice in trypanosome dilution buffer (TDB, 5 mM KCl, 80 mM NaCl, 1 mM $MgSO_4$, 20 mM Na_2HPO_4, 2 mM NaH_2PO_4, 20 mM glucose, pH 7.4), and then biotinylated strictly at 0°C and at a density of 1×10^8 cells/ml (total volume 2 ml) with 1 mM sulfo-NHS-SS-biotin (Pierce) for 10 minutes. After addition of 1 M Tris-Cl, pH 7.5, to a final concentration of 10 mM, the cells were centrifuged and taken up in 300 μl TDB. Duplicate aliquots (10 μl) were processed as follows: first, fixation in 250 μl 4% formaldehyde in 0.2 M HEPES, pH 7.4; second, addition at 0°C to a mixture of 90 μl HMI-9+iFCS and 1 ml stripping solution (18 ml RPMI medium, 9 ml water, 3 ml iFCS and 465 mg glutathione, adjusted to pH 8.5 at room temperature, then chilled on ice); third, the cells were added to 90 μl HMI-9+iFCS prewarmed to 37°C, incubated from 10 seconds to 30 minutes and then diluted with 1 ml ice-cold stripping solution. Stripping was performed for 30 minutes on ice. The cells were then collected by centrifugation (2 minutes at 8000 rpm/6000 ***g*** in an Eppendorf centrifuge), suspended in 10 μl TDB and fixed for 1 hour at 0°C in formaldehyde/HEPES. After

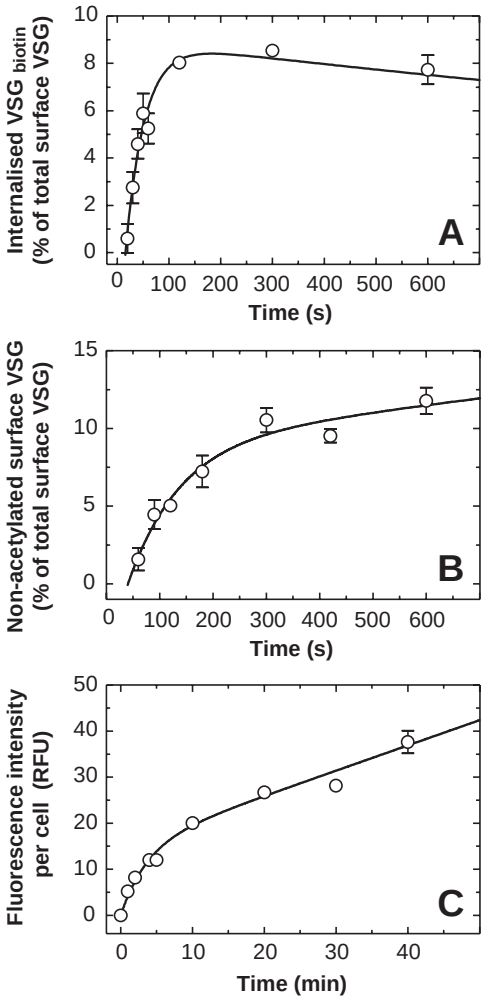

Fig. 1. Kinetics of internalisation and recycling of VSG and endocytosis of fluid-phase marker. (A) Rate of internalisation. VSG_{biotin} uptake is expressed as the fraction of surface-associated VSG_{biotin} prior to endocytosis (t=0). The data represent the average (±s.e.) of five independent experiments. (B) Rate of recycling. Exocytosis of VSG is expressed as the non-acetylated VSG transported from the cell interior to the acetylated surface normalised to the total surface VSG without treatment. The data represent the average (±s.e.) of five independent measurements. (C**)** Rate of fluid-phase uptake of Alexa Fluor 488 dextran. Internalisation is expressed as the change in relative fluorescence intensity/cell. Data from three different experiments performed at a range of concentrations (1.25 to 5 mg/ml) were normalised to 1 mg/ml and averaged.

washing in 500 μl PBS, the cells were resuspended in 50 μl PBS and permeabilised for 5 minutes at –20°C with 200 μl methanol previously cooled to this temperature. After centrifugation, the cells were processed as follows: incubation for 30 minutes in blocking solution (2% BSA/PBS/20 mM Tris-Cl/0.1% saponin, pH 7.0), addition of 200 μl Strepavidin Alexa Fluor® 488 (5 μg/ml obtained from Molecular Probes, Eugene, OR) in blocking solution, 1-hour incubation, washed once in 200 μl blocking solution, washed once in 200 μl PBS, resuspension in 0.5 ml PBS and FACS analysis (Fig. 1A).

Alternatively, the stripped cells were resuspended in 200 μl HMI-9-iFCS and fixed overnight by the addition of 300 μl 4% formaldehyde in HEPES. The cells were then washed once in 500 μl PBS, once in 500 μl PBS/2% BSA, incubated for 15 minutes in 500 μl 0.1 M Na_2HPO_4/0.1 M glycine, pH 7.2 and then permeabilised for 5

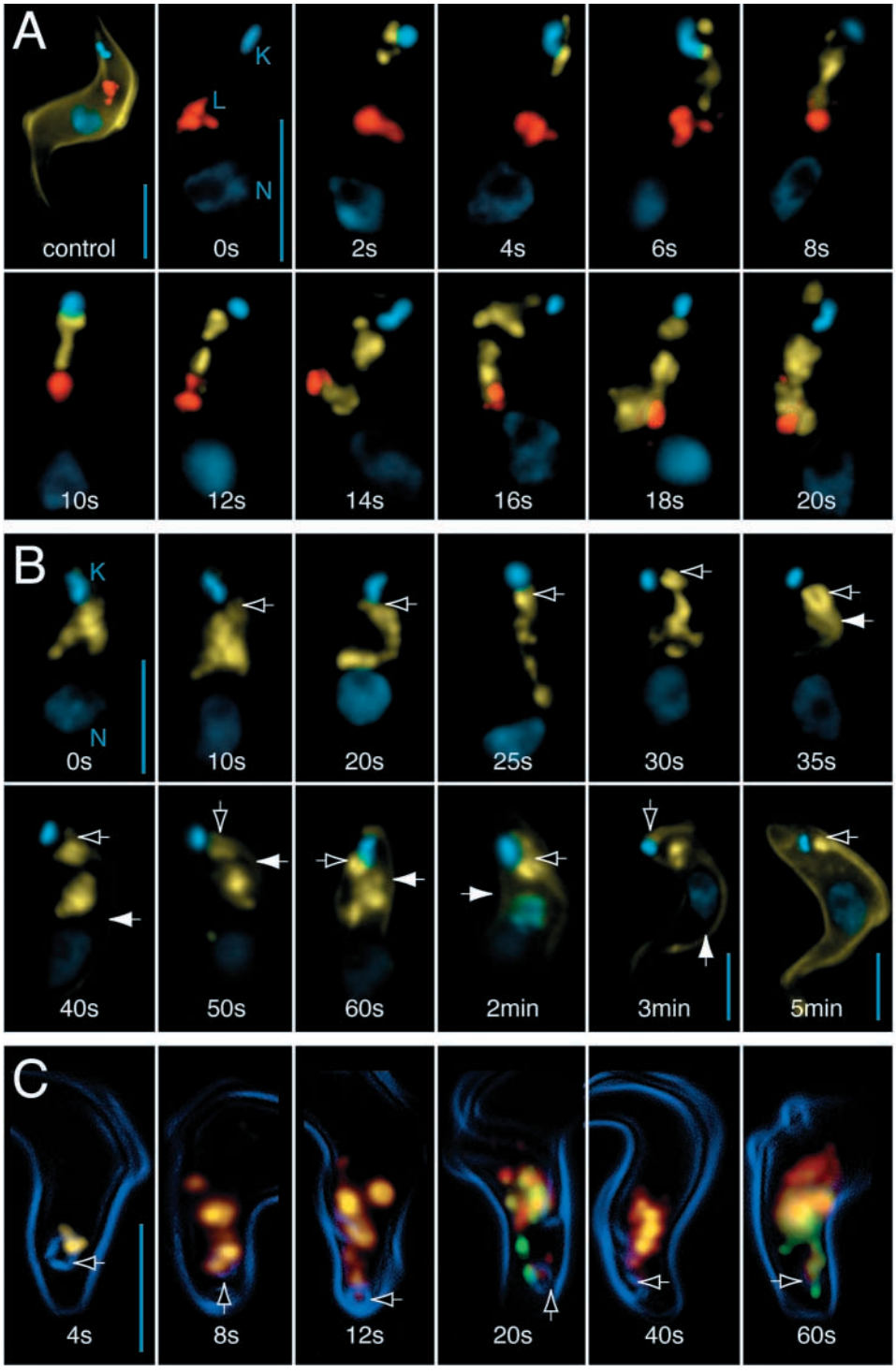

Fig. 2. Endocytosis and recycling of VSG and separation of VSG and fluid-phase cargo. Digitally deconvolved 3D-fluorescence images of representative cells at different time points are shown. (A) Kinetics of endocytosis of VSG_{biotin} at 37°C detected with Alexa Fluor 488 Streptavidin (yellow). Control refers to a surface-biotinylated cell before endocytosis. In the other samples, surface-associated biotin label has been removed prior to immuno-labelling. The lysosome (L) is marked by an anti-p67 monoclonal antibody and Alexa Fluor 594-labelled goat anti-mouse IgG (red); the kinetoplast (K) and nucleus (N) are visualised with DAPI (blue). (B) Kinetics of recycling of VSG_{biotin} (yellow). Biotinylated cells were allowed to endocytose VSG_{biotin} for 3 minutes at 37°C, then stripped of surface label at 0°C and finally incubated at 37°C for the indicated times. The flagellar pocket and the cell surface are marked by open and closed arrows, respectively. The kinetoplast (K) and nucleus (N) are visualised with DAPI (blue). (C) Kinetics of segregation of VSG_{biotin} and a fluid-phase marker. Cells were labelled at the surface with sulfo-NHS-SS-biotin and AMCA-sulfo-NHS (blue). Endocytosis was allowed in the presence of Alexa Fluor 594 dextran (red) at 37°C, the biotin label at the surface was stripped at 0°C and the cells were then processed for staining with Alexa Fluor 488 Streptavidin (green). The flagellar pocket is marked by open arrows. Blue size bars: 3 μm.

minutes by the addition of 500 μl 0.2% Triton-X-100 in PBS. After centrifugation, the cells were taken up in PBS/BSA and stained with Streptavidin Alexa Fluor as described above. As judged by cytofluorimetric analysis, the two permeabilisation protocols gave the same results. However, the second procedure was superior regarding the preservation of cell morphology.

For microscopic demonstration of VSG_{biotin} uptake (Fig. 2A), 20 μl of biotinylated cells (4×10^8/ml) were added to 180 μl of HMI-9+iFCS (37°C) and endocytosis was allowed for 0-120 seconds. The reaction was stopped by the addition of 1.8 ml of ice-cold stripping buffer (60% HMI-9, 10% iFCS, 50 mM glutathione, pH 9.0). Cells were fixed with 4% paraformaldehyde in PBS for 24 hours at 4°C and permeabilised with Triton X100 as described above. VSG_{biotin} was detected with Alexa Fluor 488 conjugated Streptavidin (10 μg/ml). For immunodetection of the lysosomal marker p67, the monoclonal antibody mAb280 (1:1000 in PBS/1% BSA; courtesy of Jay Bangs, Madison, WI) and CY3-conjugated goat anti-mouse antibody (1:2000) were used.

For co-localisation of VSG_{biotin} with endosomal markers (Fig. 3A-D), cells were incubated for 10 minutes on ice in the dark with 1 mM sulfo-NHS-SS-biotin and 1 mM AMCA-sulfo-NHS (Pierce). Endocytosis and processing for immunofluorescence were performed as described above. For each time point, aliquots of the same batch of fixed and permeabilised cells were incubated with four different antibodies. For immunodetection of RAB5A, RAB11 or clathrin heavy chain, polyclonal rabbit antisera (1:200 in PBS/1% BSA; kind gifts of Mark C. Field, Imperial College London, UK) and Alexa Fluor 488 conjugated goat anti-rabbit antibody (1:2000; Molecular Probes) were used. RAB7 was detected with a polyclonal rat antibody diluted 1:50

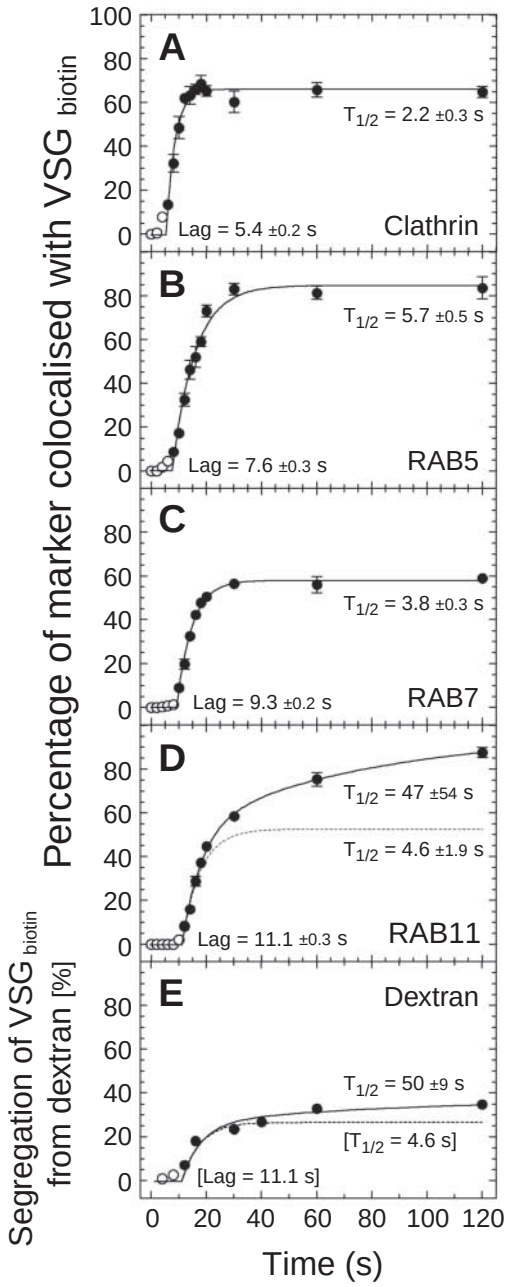

Fig. 3. Time-resolved, quantitative co-localisation analysis of VSG during endocytosis. Increase of co-localisation or of segregation in intracellular space was described empirically by first-order processes of the form $A\times(1-e^{-k\times t})$, and where this was followed by a second slower phase that derived from the first (D,E), by $A\times(1-e^{-k\times t})\times\{1+B\times[1-e^{-h\times t}]\}$. A represents the amplitude of the first phase, B is a measure for the efficiency at which A contributes to the extent of the second phase, and k and h are the rate constants. Values in brackets in E were not obtained independently from the data, but were fixed as taken from the corresponding values in D. VSG_{biotin} gains access to intracellular compartments as defined by clathrin (A), RAB5 (B), RAB7 (C) or RAB11 (D). The kinetics of the percentage of co-localisation between endocytosed VSG_{biotin} and the four markers are shown for cells taken from the same experiment. (E) Segregation of endocytosed VSG_{biotin} from Alexa Fluor 488-conjugated dextran.

(M.E. and M.B., unpublished) and Cy2-conjugated goat anti-rat IgG. For detection of VSG_{biotin}, Alexa Fluor 594 conjugated Streptavidin (10 μg/ml; Molecular Probes) was added, together with the secondary reagent.

Recycling of VSG

MITat 221-Ty-1 cells were harvested, washed and suspended at 0°C in TDB (500 μl at 5×10^8 cells/ml). Duplicate aliquots (20 μl) were either diluted with cold 200 μl HMI-9+iFCS or with 200 μl HMI-9+iFCS containing 0.5% mouse anti-VSG-NTP serum. The rest of the cells (400 μl) were mixed with 1.6 ml TDB containing 5 mM sulfo-NHS-acetate (added immediately before the cells from a freshly prepared 1 M stock solution in dimethylsulfoxide), kept for 5 minutes, treated with 20 μl 1 M Tris-Cl, pH 7.4, washed once with TDB and taken up in 400 μl TDB (all operations strictly at 0°C). Aliquots (20 μl) were either diluted with cold antibody solution or first transferred to warm Eppendorf tubes (38°C), incubated for various times and then diluted with 200 μl cold antibody solution. The cells were incubated for 30 minutes on ice, washed twice with 500 μl TDB, suspended in 10 μl TDB and fixed with 200 μl 4% formaldehyde/0.1% glutaraldehyde in 0.2 M HEPES, pH 7.4, overnight. The cells were then processed for immunofluorescence and FACS analysis using FITC-labelled goat anti-mouse $F(ab')_2$ fragments (1:100, Dianova, Hamburg, Germany). In some experiments, the mouse anti-VSG-NTP antibodies were replaced by rabbit anti-VSG-NTP serum (dilution 1:100) and Alexa-Fluor 488 goat anti-rabbit IgG (1:100, Molecular Probes). The results are shown in Fig. 1B.

For microscopic demonstration of recycling (Fig. 2B), cells that had taken up VSG_{biotin} to the steady state (3 minutes) were stripped for 5 minutes on ice with glutathione solution (pH 9.0). Aliquots of 2×10^7 cells were then added to 180 μl of pre-warmed HMI-9+iFCS, and exocytosis was allowed for 0 seconds to 5 minutes. The reaction was stopped by the addition of 1.8 ml ice-cold 4% paraformaldehyde in PBS, and immunofluorescence was performed as described.

Kinetics of fluid-phase endocytosis

Freshly harvested MITat 1.2 trypanosomes were taken up in HMI-9+iFCS at a density of 4×10^8 cells/ml and kept on ice. Duplicate samples of pre-warmed HMI-9+iFCS (45 μl), containing 0.25, 0.125 or 0.0625 mg Alexa Fluor 488 dextran conjugate (Molecular Probes, Cat. No. D-22910) and 2×10^6 cells (5 μl), were incubated for the indicated times at 37°C, diluted with 1 ml cold HMI-9+iFCS and centrifuged. The cells were washed once with 1 ml cold TDB, fixed with 4% formaldehyde/0.1% glutaraldehyde in 0.2 M HEPES, pH 7.4 for 1 hour on ice and transferred to PBS for FACS analysis. In controls, aliquots of fluorescent dextran were diluted with HMI-9 before addition of the cells. The dextran endocytosis was standardised as follows: the absorbance of a Streptavidin Alexa Fluor 488 conjugate solution (25 μg in 1 ml PBS) was determined at 493 nm. The solution was rotated overnight in the cold room with 50 μl biotin-labelled microspheres (Molecular Probes). Measurement of the absorbance of the supernatant after pelleting the beads and the bead count allowed the determination of the amount of fluorochrome bound per bead. The beads were stored in the presence of the supernatant; before use, an aliquot was centrifuged and washed twice in PBS. Fluid-phase uptake was quantified by comparing the fluorescence of the beads with that of the cells by way of cytofluorimetric analysis (Fig. 1C).

To analyse the uptake of fluid-phase cargo in relation to VSG_{biotin} endocytosis (Fig. 2C, Fig. 3E), cells labelled at the surface with biotin and AMCA were incubated at 37°C in the presence of Alexa Fluor 488 conjugated dextran (5 mg/ml), followed by cleavage of surface biotin.

Modelling of VSG internalisation and recycling, and of fluid-phase endocytosis

For internalisation of VSG, we consider a homeostatic two-step model with a bi-directional exchange of VSG, described by the rate constant k, between a pool at the cell surface, size n_s, and a pool in the endocytic compartment, size n_e. Loss of VSG, i.e. by lysosomal degradation or, in the case of VSG_{biotin}, by loss of the biotin label occurs with a rate constant k_d. Biosynthesis of VSG is described by a rate constant k_b. When VSG at the cell surface is biotinylated, it will be exchanged between n_s and n_e and a steady-state distribution will be established.

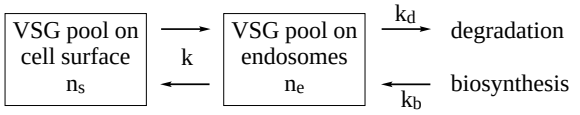

We determined the time course of transport VSG_{biotin} to the endosomal compartment, n_e*, measured as a fraction of the amount of cell surface VSG, n_s, namely n_e*/n_s. When a concentration-dependent exchange rate of VSG_{biotin} is assumed (i.e. a first-order process), this process can be described by:

$$n_e \times (t)/n_s = A \times [1 - e^{-K \times (t-L)}] \times e^{-Kd \times (t-L)}, \quad (1)$$

where $A=n_e/(n_s+n_e)$ (%), $K=k\times(1/n_s+1/n_e)$ (1/s), $Kd=k_d/(2\times n_e)$ (1/s), $k_b=0$ (because biosynthetic VSG is not biotinylated), and L=lag after cooling (seconds).

The same model can be used for analysis of recycling of non-acetylated VSG from endosomes, n_e*, to the cell surface, n_s*, as given by:

$$n_s \times (t)/n_s = A \times e^{-Kb \times (t-L)} \times [1 - e^{-K \times (t-L)}] + [1 - e^{-Kb \times (t-L)}], \quad (2)$$

where the symbols have the same meaning as above, $Kb=k_b/(2\times n_e)$ and $k_d=0$ because degradation of acetylated VSG does not affect the signal. All fittings were performed using the Prism 3 software (Graphpad, San Diego, CA).

The uptake of the fluid-phase marker Alexa Fluor dextran into the endocytic compartment is characterised by the uptake rate constant, k_i [$\mu m^3 \times (cell \times minute)^{-1}$], whereas the rate of release into the flagellar pocket/medium is described by the rate constant k_o and the rate of net fluid-phase uptake into the lysosome by the rate constant $k=(k_i-k_o)$ [$\mu m^3 \times (cell \times minute)^{-1}$].

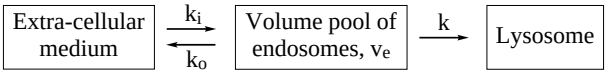

The time course for the accumulation of fluid-phase marker in the cell is then given by:

$$n(t) = (c \times k_i)/\lambda \times \{(1 - e^{-\lambda \times t}) \times (1 - k/[k_o + k]) + t \times k/v_e\}, \quad (3)$$

where $n=(n_e+n_{Ly})$ (mole $cell^{-1}$) corresponds to the sum of marker in endosomes and lysosomes, v_e (μm^3 $cell^{-1}$) is the volume of the endosome compartment, c is the extracellular concentration of the fluid-phase marker, and $\lambda=(k_o+k)/v_e$.

Image acquisition, deconvolution and quantitative co-localisation analysis

Three-dimensional image acquisition, digital deconvolution and image analysis was performed as described (Grünfelder et al., 2003). Briefly, a motorized Zeiss Axiophot2 widefield microscope, a PIFOC objective z-stepper and either the Princeton Instruments 'Micromax' cooled slow-scan CCD camera (KAF-1400 chip) or the CoolSnap HQ cooled CCD camera (Sony ICX285 chip) were used for image acquisition. Following deconvolution with the Huygens Professional software (Scientific Volume Imaging, Hilversum, The Netherlands), the restored image dataset was analysed using the Imaris Surpass software package (Bitplane, Zurich, Switzerland). Co-localisation analysis of deconvolved 3D-images was performed with the colocalisation software (version 1.0, Bitplane). Throughout the experiments, the selection of cells for analysis was done 'blindly' without knowing the identity of the sample. Furthermore, the identification of representative cells was performed by applying customised software scripts (based on IPLab, Scanalytics, Fairfax, VA) that segment, classify and rank all objects (cells) within an image, resulting in a colour-coded overlay. This ensured that only cells that revealed the predominant phenotype were analysed.

Results

Kinetics of endocytosis and recycling of VSG

Trypanosomes expressing VSG 221 (variant clone MITat 1.2) were surface biotinylated by using the impermeable reagent sulfo-succinimidyl-2-(biotinamido)-ethyl-1,3-dithiopropionate (sulfo-NHS-SS-biotin). Under our labelling conditions, >95% of all biotin label is associated with VSG (VSG_{biotin}) (Grünfelder et al., 2002). The cells were incubated for various times at 37°C to allow endocytosis to proceed and then the surface-associated biotin was stripped by an excess of glutathione at 0°C and pH 8.5. The cells were fixed, permeabilised, labelled with fluorescent Streptavidin and analysed by flow cytometry. The time course of endocytosis for VSG_{biotin} from the cell surface to endosomal membranes is shown in Fig. 1A. After a short lag (16 seconds), the cells rapidly internalised VSG_{biotin}, leading to a steady-state after approximately 2 minutes. Thereafter, a slow decrease was observed, possibly because of the removal of biotin label by disulfide reduction in late endosomes (Fivaz et al., 2002). The curve describes the best fit of a two-step kinetic model, consisting of the reversible flow of VSG between the surface and the endocytic compartment, and an endosomal degradation step that leads to a loss of the signal (see Eqn 1). Values for the following parameters could be obtained from this simulation: (1) At steady state, 8.9±0.6% of the total VSG_{biotin} was located in the endosomal compartment, with the complementary fraction of 91.1% being on the cell surface. (2) VSG exchange between the cell surface and an intracellular pool could be described by a bi-directional rate constant of 0.145±0.04 surface equivalents of VSG per minute; thus, one surface equivalent was internalised every 7±1.8 minutes, or one VSG equivalent of the endosomal compartment was recycled every 0.7 minutes. (3) Biotin label was lost from the cells with a half-life of 3.6±1.1 hours.

Recycling of VSG_{biotin} after endocytosis could be demonstrated during a second incubation of the stripped cells at 37°C by fluorescence microscopy (see below). However, we were unable to obtain reproducible quantitative data using this technique, most probably because of the stressful stripping conditions. Therefore, we resorted to the following procedure: Strain MITat 221-Ty-1 expresses a mutant *vsg 221* gene, with the yeast Ty-1 epitope tag inserted close to the N-terminus (NH_2-AAEKG*AR***EVHTNQDP***LD*KQAFWQPLC-; tag in bold letters, amino acid changes because of cloning in italics), whereas the WT *vsg 221* gene has been deleted (M.E., unpublished). This modified VSG was recognised by anti-peptide antibodies to the N-terminus of VSG 221 on live trypanosomes and, moreover, most of this reaction could be abolished by treating the cells with the membrane-impermeable acetylation reagent N-hydroxysulfosuccinimide

acetate (sulfo-NHS-acetate). Therefore, MITat 221-Ty-1 cells were acetylated at 0°C, then incubated at 37°C for different times, fixed, labelled using the anti-peptide and secondary antibodies and then subjected to flow cytometric analysis. The time course for the redistribution of the non-acetylated VSG from endosomes to the cell surface is shown in Fig. 1B. Simulation of the data with the same two-step model as described above (but taking the biosynthesis of VSG into account) (see Eqn 2) yielded values for the following parameters: (1) The relative pool size of VSG in endosomes was 9.1±3.2% of the total cell-associated VSG. (2) Bi-directional exchange occurred with a rate constant of 0.056±0.034 surface equivalents per minute; thus, one surface equivalent of VSG was recycled every 18±11 minutes, or one VSG equivalent of the endosomal compartment was recycled every 1.8 minutes. (3) The biosynthesis of VSG contributed to the non-acetylated VSG pool and led to an increase in signal that doubled with a half time, $t_{1/2}$=21±32 hours.

Kinetics of fluid-phase endocytosis

The time course of fluid-phase uptake of Alexa 488 dextran conjugate by trypanosomes is shown in Fig. 1C. Uptake was linearly dependent on the dextran concentration (data not shown). After normalising uptake values to the same dextran concentration, the averaged results could be simulated by a two-step model, comprising a reversible uptake step into endosomes as characterised by forward and backward rate constants, k_i and k_o, respectively, and a rate constant $k=k_i–k_o$ for the transfer of the dextran from endosomes to the lysosome (see Eqn 3). These kinetics describe fluid uptake at a rate k_i=0.19±0.03 μm^3 (cell minute)$^{–1}$ and the release of marker at a rate k_o=0.17±0.026 μm^3 (cell minute)$^{–1}$. Therefore, the net uptake occurred at a rate k=0.02±0.002 μm^3 (cell minute)$^{–1}$; i.e. only approximately 10% of the pinocytosed marker was retained by the cells (see change in slope in the uptake curve in Fig. 1C). The marker filled an endosomal volume, v_e=0.69±0.08 μm^3 cell$^{–1}$ with a turnover time of $\tau=v_e/k_i$=3.6 minutes. It should be noted that previous estimates for the rate of endocytosis by Fairlamb and Bowman (Fairlamb and Bowman, 1980) [0.01 μm^3 (cell minute)$^{–1}$ at 25°C] and Coppens et al. (Coppens et al., 1987) [0.017 μm^3 (cell minute)$^{–1}$ at 30°C] can now be assigned to the net rather than the 10 times faster initial rate of uptake.

The itinerary of VSG through the endosomal system

The flow of VSG_{biotin} through the endosomal system was studied by 3D deconvolution fluorescence microscopy and is presented in two ways. First, the different stages of endocytosis, recycling and the separation of VSG_{biotin} from dextran as fluid-phase marker are shown for representative cell images in Fig. 2A-C. Second, a time-resolved, quantitative co-localisation analysis is presented in Fig. 3, which was performed as follows: the cellular space occupied by a given marker was expressed as an ensemble of volume units (voxels of 41×41×50 nm^3) and was measured after having defined a threshold for the detection of VSG_{biotin} above background fluorescence (signal strength, in general, at least 50 times above background). With the help of automated, stringent image segmentation and classification techniques it was ensured that the sampled cells were representative and comparable for a given population based on three criteria: (1) Only non-dividing cells were analysed, (2) the summed fluorescence intensity of all three image channels was equal, and (3) sampled cells were comparable in terms of the overall size of the compartment analysed. The graphs in Fig. 3A-D describe the kinetics of appearance and subsequent spreading of internalised VSG_{biotin} in a given marker-defined compartment. It has to be pointed out, that these data do not quantify the amount of VSG_{biotin} within a compartment and, therefore, they do not provide information on the flux of VSG_{biotin}, i.e. major and minor routes cannot be distinguished. Specific antibodies against clathrin (Morgan et al., 2001; Grünfelder et al., 2003) and three small GTPases (1) RAB5A, a marker for early endosomes (Pal et al., 2002; Chavrier et al., 1990), (2) RAB7, a marker for late endosomes (M.B., unpublished) (Chavrier et al., 1990), and (3) RAB11, a marker for recycling endosomes (Jeffries et al., 2001; Grünfelder et al., 2003) were used in this analysis.

Comparison of a cell biotinylated at 0°C (control) and a cell subsequently treated with glutathione at 0°C (0 seconds) confirmed that surface biotin was completely removed, also from the flagellar pocket membrane (Fig. 2A). Internalised VSG_{biotin} was detectable at the flagellar pocket only 2 seconds after initiation of endocytosis. Interestingly, VSG_{biotin} was then routed straight towards the lysosomal area, which was reached within 6-10 seconds. Co-localisation analysis with the lysosomal marker p67 demonstrated that VSG_{biotin} did not enter the lysosome, but was redirected back towards the flagellar pocket. After 40-50 seconds, a steady state in the spatial distribution of VSG_{biotin} between flagellar pocket and lysosome was reached.

After a short lag, which may be attributed to the recovery of the cells from cooling, VSG_{biotin} became rapidly ($T_{1/2}$=2.2 seconds) associated with clathrin-containing structures (Fig. 3A). The kinetics of spreading into the clathrin-containing space was compatible with a first-order process. At steady state, which was reached after approximately 15 seconds, VSG_{biotin} co-localised with 65% of the cell-associated clathrin. We propose that the remaining 35% of the clathrin-containing space consisted mainly of VSG-free class II clathrin-coated vesicles that budded from endosomes (Grünfelder et al., 2003). By 2.2 seconds after entry into the clathrin compartment, VSG_{biotin} started to co-localise with RAB5A, the marker for early endosomes. This compartment was filled with a $T_{1/2}$=5.7 seconds to 85%, suggesting that VSG_{biotin} traversed almost all of the RAB5A-positive space (Fig. 3B). After a further delay of approximately 2 seconds, VSG_{biotin} became detectable in late endosomes as indicated by its co-localisation with RAB7 ($T_{1/2}$=3.8 seconds) (Fig. 3C), and, at steady state, occupied only 58% of this compartmental space. This indicated that a substantial fraction of the RAB7-positive space did not lie on the intracellular route of VSG and probably represented a later stage of late endosomes at which segregation between VSG_{biotin} and the fluid-phase cargo may have occurred already. Finally, at approximately 6 seconds after the onset of uptake (i.e. a lag of 11.1 seconds) (compare Fig. 3A with Fig. 3D), VSG_{biotin} entered RAB11-containing structures with biphasic kinetics: the first phase occurred with a $T_{1/2}$=4.6±2 seconds, a time course similar to that found for VSG_{biotin} entering the RAB7-positive space. Although this process filled 53% of this

space at steady state, the remaining 47% became populated with a $T_{1/2}$=47±50 seconds, presumably representing a second and later stage for the production of VSG-containing recycling endosomes.

The uptake of fluorescently labelled dextran was followed in cells that were dually labelled at the surface with cleavable biotin and non-cleavable sulfo-succinimidyl-7-amino-4-methylcoumarin-3-acetic acid (AMCA-sulfo-NHS) (Fig. 2C). After stripping, the biotin signal was specific for endocytosed VSG_{biotin}. Although VSG_{AMCA} was also endocytosed (Grünfelder et al., 2003), its fluorescence was quenched in endosomes and this label was therefore specific for surface-exposed VSG_{AMCA}. Dextran was endocytosed together with VSG_{biotin} (yellow regions in Fig. 2C), however, thereafter it gradually segregated from internalised VSG_{biotin}, and reached a maximum of spatial separation after approximately 1 minute. Co-localisation with the lysosomal marker p67 revealed that dextran accumulated within the lysosome (data not shown). A quantitative analysis of the segregation of VSG_{biotin} and dextran is shown in Fig. 3E. The data suggest that at steady state 37% of the intracellular VSG_{biotin} did not lie on the endocytic route of internalised dextran. Of this 37%, 26±4% segregated from dextran with a $T_{1/2}$=4.6 seconds (broken line), whereas the remaining 11±4% segregated with a $T_{1/2}$=50 seconds. Because the lag (11.1 seconds) as well as both half times of VSG/dextran segregation were compatible with the time course of filling of the RAB11 compartment, we suggest that the separation of VSG from the fluid-phase marker occurred concurrently with the biphasic filling of the RAB11 space.

In an additional experiment, the exocytosis of VSG_{biotin} from the endosomal compartment was studied (Fig. 2B). VSG_{biotin} filled the flagellar pocket within 10-25 seconds, and after 30 seconds appeared on the pellicular cell surface. This was confirmed by specifically measuring cell surface VSG_{biotin} in non-permeabilised cells (data not shown). Within 2 minutes of exocytosis, the endocyctic compartment was emptied, and by 5 minutes biotinylated VSG was distributed over the cell surface.

Defining endosomal compartments

Fig. 4D summarises our present view of endosomal structures in *T. brucei* as deduced from recent microscopic and immunoelectron microscopic studies (Morgan et al., 2001; Jeffries et al., 2001; Grünfelder et al., 2003), as well as on new assignments in the present study that are based on the reactivity of antibodies against RAB5A and RAB7.

The ultrastructural evidence (see Grünfelder et al., 2003) and the phenotype of a conditional mutant where clathrin or epsin was downregulated by RNA-interference (M. Günzel and M.E., unpublished) strongly suggest that endocytosis occurs exclusively by way of class I clathrin-coated vesicles (CCVs, 135 nm in diameter) (Grünfelder et al., 2003), which bud from the flagellar pocket membrane.

In immunofluorescence, antibodies against RAB5A reacted with structures close to the lysosome (Fig. 4A). By evaluating 250 random cryosections in the electron microscope, 74% of the RAB5A-immuno gold label was associated with cisternal and vesicular profiles close to the lysosome, whereas the rest was associated with structures between the flagellar pocket and the nucleus. At least half of the labelled cisternae had circular profiles (cEC) (Fig. 4E). The cECs showed class II clathrin-coated budding structures. No RAB5A was detectable on the flagellar pocket membrane, the cell surface, extended cisternae (EC) corresponding to RAB11-positive recycling endosomes (Fig. 4E) and the RAB11-positive exocytic carrier vesicles (EXCs) (Fig. 4E). The circular endosomal profiles identified here as early endosomes resembled those observed in mammalian cells (Griffiths et al., 1989).

In immunofluorescence, antibodies against RAB7 labelled structures near the lysosome (Fig. 4B) in an area that was closely juxtaposed but distinct from the RAB5A-reactive area (Fig. 4C). On cryosections, these antibodies reacted specifically, but weakly with membrane structures adjacent to the lysosome. Occasionally, strongly positive, irregularly shaped, complex membrane structures (0.5-1 μm diameter) were observed (Fig. 4F) that resembled late endosomes in mammalian cells (Griffiths et al., 1989). Extended cisternae were negative for RAB7.

As shown before (Grünfelder et al., 2003), RAB11-positive EC and EXCs were found throughout the posterior half of the cell. We have suggested that these cisternae disintegrate into EXCs, which then fuse with the flagellar pocket membrane.

The ultrastructure of endosomes of *T. brucei* labelled by ferritin or horseradish peroxidase (HRP) as fluid-phase markers has been described in detail (Langreth and Balber, 1975; Webster, 1989). The definition of endosomal sub-compartment justified an extension of those studies (Fig. 4G-I). As expected, class I CCVs were labelled by both markers (see for HRP in Fig. 4G). Remarkably, ferritin (size 11 nm) was excluded from the narrow parts of circular cisternal profiles (cEC), EC (Fig. 4I) and EXCs. The exclusion of ferritin or transferrin-gold complexes from narrow cisternal structures has previously been observed by Langreth and Balber (Langreth and Balber, 1975) and Webster and Grab (Webster and Grab, 1988). Likewise, LDL particles are excluded from narrow cisternal or tubular endosomal structures in mammalian cells (Ghosh et al., 1994). In contrast, all of these structures were positive for the much smaller protein HRP (44 kDa) (Fig. 4G,H). The fact that HRP was present in EXCs suggested that this fluid-phase marker was recycled to the flagellar pocket. Importantly, incipient or free class II CCVs were strongly labelled by either HRP or ferritin (Fig. 4G-I). Because these vesicles budded from circular and extended cisternal profiles and, eventually, both ferritin and HPR ended up in the lysosome, we suggest that class II CCVs carry fluid-phase markers to late endosomes or to the lysosome or both.

Discussion

Rates of VSG and fluid-phase endocytosis

The results for both the internalisation and the recycling of VSG in trypanosomes are compatible with a kinetic model for the overall homeostatic VSG exchange between the cell surface and an endosomal membrane pool. At steady state, the intracellular pool of VSG amounts to 9±4% of the total cell-associated VSG. This result is in reasonable agreement with previous estimates obtained by fluorescence (4.9%) or by immunoelectron microscopy (6.2%) (Grünfelder et al., 2002). The averaged rate of internalisation and recycling of VSG

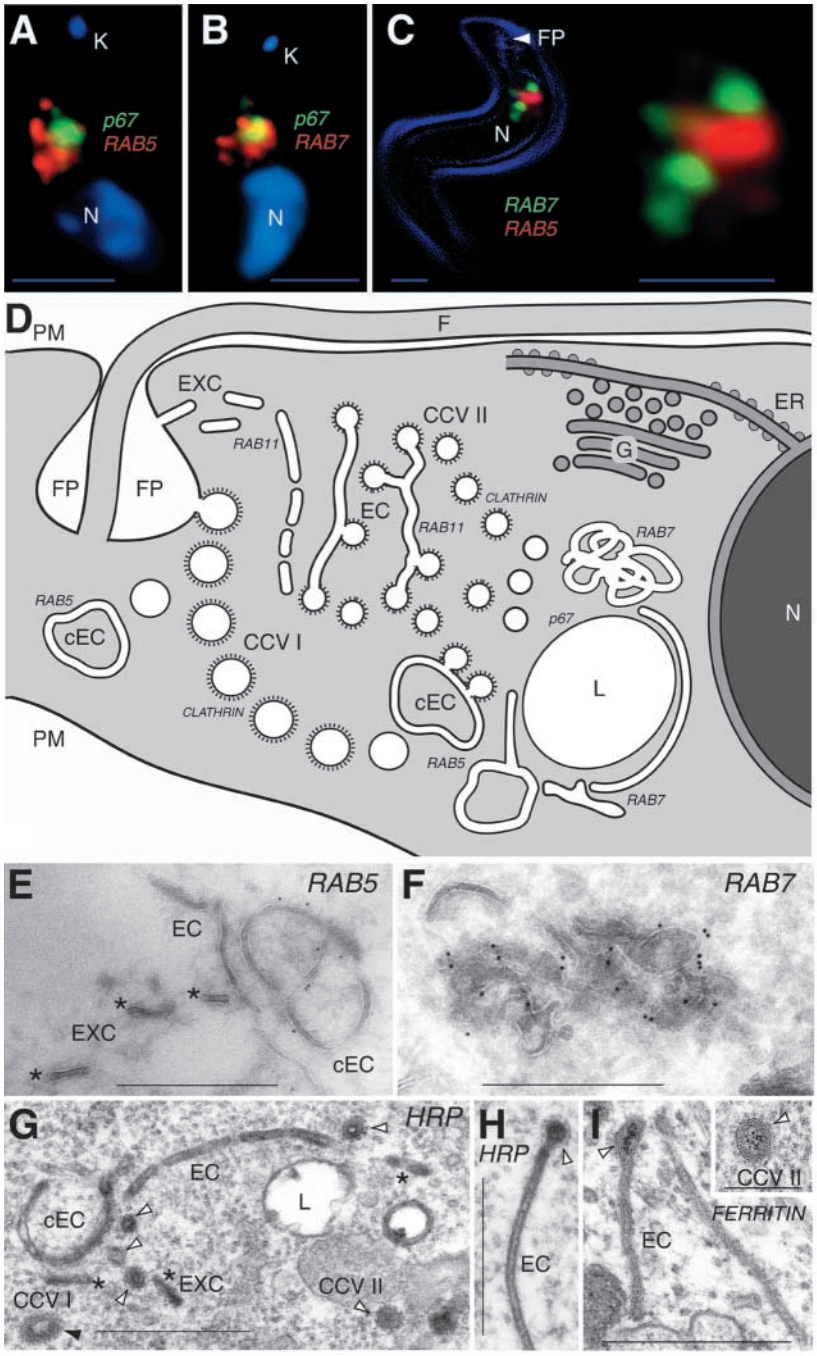

Fig. 4. Endosomal compartments of *T. brucei*. A-C show deconvolved 3D immunofluorescence images of cells labelled with primary and fluorophore-tagged secondary antibodies. (A) The RAB5A-positive compartment stained by rabbit antibodies (red) is located close to the lysosome (labelled by a mouse antibody against p67; green). The kinetoplast (K) and nucleus (N) are visualised by DAPI. (B) The RAB7-positive compartment stained by rabbit antibodies (red) is located close to the lysosome (labelled by p67; green). 3D inspection indicates that the two compartments do not overlap. (C) Visualisation of the RAB7-compartment with rat antibodies (green) and the RAB5A-compartment with rabbit antibodies (red) shows that the two compartments are closely associated but distinct. The cell surface and flagellar pocket are labelled by AMCA (blue). (D) Schematic diagram of endocytic structures. (E) Electron micrograph of cryosection labelled with rabbit-anti-RAB5A antibodies and 6 nm Protein A-gold complexes. cEC is positive, whereas linear EC and EXCs (asterisks) are not labelled. (F) Cryosection labelled with rat anti-RAB7 antibodies and goat anti-rat IgG/IgM-12 nm gold conjugate. The antibodies bind to a complex membrane structure. (G) Cells were incubated for 3 minutes at 37°C in the presence of 10 mg/ml horseradish peroxidase (HRP) and processed for diaminobenzidine-staining and Epon embedding (Webster, 1989). The enzyme is detected in cisternae (EC and cEC), class I (filled arrow head) and class II CCVs (open arrow heads) and in EXCs (asterisks). (H) Same as G. A class II CCV (arrow head) budding from the rim of an EC is strongly labelled. (I) Cells were incubated for 5 minutes at 37°C with ferritin (50 mg/ml) and then processed for Epon embedding (Langreth and Balber, 1975). Ferritin is excluded from the narrow luminal parts of the cisternae but present in abundance in clathrin-coated buds (arrow head) and in class II CCVs (inset). CCV I, class I clathrin-coated vesicle; CCV II, class II clathrin-coated vesicle; cEC, circular endosomal profiles; EC, endosomal cisterna; ER, endoplasmic reticulum; EXC, exocytic carrier; F, flagellum; FP, flagellar pocket; G, Golgi complex; K, kinetoplast; L, lysosome; N, nucleus; PM, plasma membrane. Bars: A-C, 2 μm; E-I, 0.5 μm; I (inset), 0.2 μm.

amounts to 8±4% VSG surface-equivalents per minute, implying that the entire surface pool is internalised and recycled once in approximately 12.5 minutes (Table 1). Because the intracellular VSG pool is approximately ten-times smaller, its turnover requires only approximately 1 minute.

A trypanosome takes up fluid at a rate of 0.19±0.03 μm^3 (cell minute)$^{-1}$ (Fig. 1C) into an endosome volume of 0.69±0.08 μm^3 cell^{-1}. This implies that the entire endosome volume is filled once approximately every 3.6 minutes. Because the lumen of endocytic vesicles (without the VSG coat) is approximately 0.1 μm in diameter, a volume of 0.69 μm^3 corresponds to approximately 1350 vesicles with a combined surface area of approximately 42 μm^2. Therefore, membrane is internalised at a rate of 42/3.6=11.7 μm^2/minute. The estimate for the volume of the endosomal compartment is in reasonable agreement with stereologically determined, lower estimates of approximately 1 μm^3 (Grünfelder et al., 2002). It is reassuring that the internalisation rate of 11.7 μm^2/minute, which is based on surface to volume considerations, agrees with an averaged value of 11.5 μm^2/minute obtained by relating the internalisation rate of VSG (8%/minute) to the surface area of 144 μm^2 (Grünfelder et al., 2002). Therefore, internalisation of VSG is representative for the rate of membrane internalisation. This is in agreement with our previous observation that endocytosis of VSG in class I clathrin-coated vesicles occurs without a change in lateral concentration compared with the flagellar pocket membrane (Grünfelder et al., 2003). In contrast, a comparison between the time it takes to turn over one area equivalent of

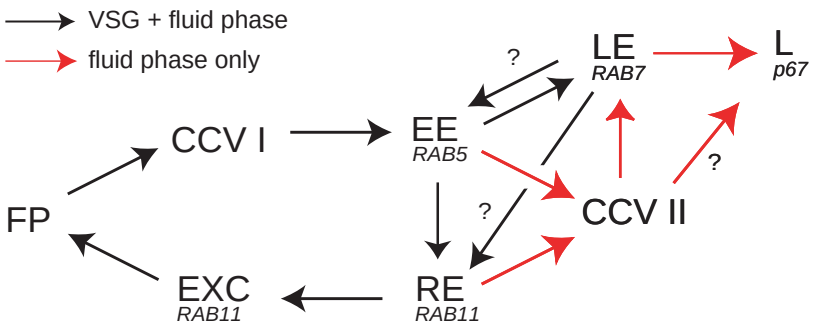

Fig. 5. Flow diagram of VSG or fluid-phase cargo through endosomal structures. CCV I and II, clathrin-coated vesicles of classes I and II; EE, early endosome; EXC, exocytic carrier; FP, flagellar pocket; L, lysosome; LE, late endosome; RE, recycling endosome. The markers defining these compartments are indicated.

endosome membrane of >28.3 μm^2 (Grünfelder et al., 2002) by a membrane flux of 11.7 μm^2/minute, namely >2.4 minutes, and the time it takes to turn over one VSG equivalent of this compartment (approximately 1 minute, see above), implies that the VSG density is >2.4-fold less in endosomes than on the cell surface. In rough agreement with this estimate, we previously concluded using immuno-gold electron microscopy that, on average, the VSG density in endosomes is 4.8-fold less than on the plasma/flagellar pocket membrane (Grünfelder et al., 2002).

The rate of endosome volume turnover in *T. brucei* is 1.5 to 3.1 times faster than in macrophages or fibroblasts. *T. brucei* turns over its cell surface 2.6 times faster than macrophages and 5-9 times faster than fibroblasts (as an average from several studies) (for a review, see Thilo, 1985) (see Table 1 for direct comparison with data from two specific studies). This rate turns out to be exceptionally high when it is considered that membrane internalisation occurs only from a specialised surface domain, the flagellar pocket, that is, one surface area equivalent is internalised through only 1/20th of this area in 12.5 minutes. Because endocytosis appears to occur exclusively via clathrin-coated vesicles, this implies that 6-7 class I CCVs (4% of the total pocket area) are internalised every second. Qualitatively, this result is consistent with the abundance of these vesicles within the cell as identified in electron microscopic sections of trypanosomes after short incubation times with HRP. However, at steady state only two clathrin-coated pits per flagellar pocket are present (C.G.G., unpublished), suggesting that their life time is significantly shorter than in mammalian cells (20-80 seconds) (Gaidorov et al., 1999). The restriction of endocytosis to the flagellar pocket membrane of *T. brucei* is reminiscent of the recently described, specialised endocytic zones of neuronal dendrites and spines (Blanpied et al., 2002). However, even at these hot spots of endocytosis, clathrin assembly occurs with an average time constant of 19 seconds, which is slower than in the parasite. This suggests unique features of coated vesicle formation, one of which may be the absence of the adaptor complex AP-2 that is the second major structural protein of coated pits in mammalian cells (Morgan et al., 2002b).

Endocytosis may be important for removing anti-VSG antibodies from the cell surface (Russo et al., 1993; O'Beirne et al., 1998); that is, up to a certain antibody level in the blood, the parasites may be able to evade Fc-receptor-mediated phagocytosis by macrophages. In fact, quantification in vitro of the rate of antibody endocytosis/degradation shows remarkably rapid kinetics of anti-VSG-IgG endocytosis (M.E., unpublished). Therefore, the high rate of endocytosis may contribute to the persistence of *T. brucei* in the vascular system of mammals.

Table 1. Membrane and volume turnover in *Trypanosoma brucei* and mammalian cells

Cell type	*T. brucei*	Peritoneal macrophage*	Baby hamster kidney cell†	Fibroblast L-cell*
Plasma membrane turnover (min)	7±1.8‡ 18±11§ 12.5 (average)	32	63	115
Endosome membrane turnover (min)	>2.4	3.8	12.3	4.7
Endosome volume turnover (min)	5.3¶ 3.6**	8	14	6.5

Based on VSG data on the assumption that plasma membrane is internalised without a change in surface concentration of VSG, i.e. VSG is representative of total plasma membrane during internalisation. This is not true of endosomal membranes, but the internalisation rate of 0.19 μm^2/s can be divided into the sterologically determined endosomal membrane area (>28.3 μm^2) (Grünfelder et al., 2002) to calculate the turnover time for the endosome membrane pool.

*Steinman et al., 1976.

†Griffiths et al., 1989.

‡Based on the rate of VSG_{biotin} internalisation.

§Based on the VSG recycling rate.

¶Based on the rate of fluid phase uptake and the sterologically determined endosome volume (~1 μm^3 cell^{-1}) (Grünfelder et al., 2002).

**Based on the rate of fluid phase uptake and the measured endosome volume (0.69±0.08 μm^3 cell^{-1}).

Pathway of VSG through the endocytic system

The information on the trafficking of VSG and of fluid-phase cargo through the endocytic system of *T. brucei* is summarised schematically in Fig. 5 (compare also Fig. 4D). We would like to argue that the fraction (66%) of the clathrin-containing compartment that receives VSG within 10 seconds after the start of endocytosis (Fig. 3A) corresponds to class I CCVs. These vesicles move towards the region of the lysosome, where they deliver VSG and fluid-phase marker to essentially all RAB5-positive early endosomes (Fig. 2A and Fig. 3B). Therefore, we propose that early endosomes are an obligatory station on the intracellular path of VSG. Kinetic experiments based on electron microscopy have confirmed that VSG_{biotin} and the fluid-phase marker HRP become rapidly associated with circular profiles of EC (C.G.G., unpublished).

An interpretation of the VSG pathway between the early

endosomes and the RAB11-positive exocytic carriers, which eventually deliver VSG back to the flagellar pocket membrane, is less straightforward. Approximately 2 seconds and 6 seconds after its first appearance in the RAB5-positive compartment, VSG becomes associated with 58% of the RAB7- and 53% of the RAB11-positive compartments, respectively, with similar half lives (Fig. 3C,D). The same half life is also compatible with the rate at which a fraction of the VSG separates from the fluid-phase marker (Fig. 3E), suggesting that all three of these half lives describe different aspects of the same process. In contrast to VSG, the fluid-phase marker has access to the entire RAB7-positive compartment (data not shown). Therefore, part of the VSG appears to move directly from early endosomes to recycling endosomes in a first stage of sorting and recycling, whereas the remainder moves on to late endosomes. This is then followed by a second and slower phase of VSG recycling from the late endosomes to recycling endosomes, which appears to occur concomitantly with the separation between VSG and content marker because both processes occur with half lives, $T_{1/2}$=47-50 seconds. The fluid-phase marker could subsequently be delivered from late endosomes to the lysosome.

We have previously shown that VSG is depleted in the class II CCVs that bud from EC, suggesting that in this way VSG is concentrated in the cisternae by negative selection. Accordingly, class II CCVs are also depleted of endocytosed VSG_{biotin} (C.G.G., unpublished). Importantly, these vesicles have now turned out to be strongly positive for ferritin or HRP (Fig. 4G-I). In mammalian cells, similar endosome-derived CCVs have generally been considered to be directed towards the plasma membrane (Stoorvogel et al., 1996; Futter et al., 1998) (see also Sönnichsen et al., 2000). Instead, we would like to propose that at least for the *T. brucei* system they carry cargo to late endosomes or directly to the lysosome or both. As judged by either fluorescence or by electron microscopic evidence, neither the lysosome nor the Golgi complex are stations in the recycling pathway of VSG. Similarly, cell surface-derived glycoproteins on endosomes of macrophages are efficiently recycled at two pre-lysosomal stages (Thilo et al., 1995) without reaching the lysosomal membrane (Haylett and Thilo, 1986).

In mammalian cells, GPI-anchored proteins have been shown to enter via clathrin-independent pathways and are routed thereafter to a special GPI-anchored-protein-enriched endosomal compartment (GEEC), to late or recycling endosomes or to the Golgi complex (Skretting et al., 1999; Nichols et al., 2001; Sabharanjak et al., 2002; Fivaz et al., 2002). Their intracellular trafficking appears to depend on the cell type as well as on the specific GPI-anchored protein under investigation, and, at several stations, the importance of cholesterol- and sphingolipid-rich domains have been implicated in their sorting (see Sharma et al., 2002). The endocytic recycling pathway for the GPI-anchored VSG in trypanosomes is comparatively straightforward: entry and exit at the flagellar pocket are defined; no special intracellular compartments have to be invoked, and sorting appears to occur by negative selection in endosomes.

The present study poses several questions that should be addressed in the future. First, how is the endo- and exocytic traffic spatially regulated in the flagellar pocket? Is its membrane functionally uniform or is it divided in sub-regions, which either support clathrin-mediated endocytosis or fusion of exocytic carriers? Second, although the membrane area of disk-shaped exocytic carriers is comparable to that of the class I CCVs, their luminal volume is much smaller. Therefore, if 90% of the fluid-phase marker is recycled, it must either be concentrated in the exocytic carriers or there exists an unknown recycling route. Third, the relationship of the RAB5- and the RAB11-positive cisternae can be analysed in more detail. As discussed for mammalian cells, these compartments may rapidly communicate by fusion/fission events or even be continuous (Sönnichsen et al., 2000). Therefore, although the molecular description of the endocytic pathway in trypanosomes at this stage is still rudimentary when compared with that of mammalian cells or yeast, the advantages of the parasite system merit further investigations.

We thank Mark Field (London) and Jay Bangs (Madison) for their generous supply of antibodies. We are grateful to Mark Carrington (Cambridge, UK) and Paul Webster (New Haven) for helpful discussions. M.E. and M.B. acknowledge the support of the Deutsche Forschungsgemeinschaft, P.O. thanks the Fond der Chemischen Industrie for its support.

References

Alexander, D. L., Schwartz, K. J., Balber, A. E. and Bangs, J. D. (2002). Developmentally regulated trafficking of the lysosomal membrane protein p67 in *Trypansoma brucei*. *J. Cell Sci.* **115**, 3253-3263.

Blanpied, T. A., Scott, D. B. and Ehlers, M. D. (2002). Dynamics and regulation of clathrin coats at specialized endocytic zones of dendrites and spines. *Neuron* **36**, 435-449.

Chavrier, P., Parton, R. G., Hauri, H. P., Simons, K. and Zerial, M. (1990). Localization of low molecular weight GTP binding proteins to exocytic and endocytic compartments. *Cell* **62**, 317-329.

Coppens, I., Opperdoes, F. R., Courtoy, P. J. and Baudhuin, P. B. (1987). Receptor-mediated endocytosis in the bloodstream form of *Trypanosoma brucei*. *J. Protozool.* **34**, 465-473.

Fairlamb, A. H. and Bowman, I. B. (1980). *Trypanosoma brucei*: maintenance of concentrated suspensions of bloodstream trypomastigotes in vitro using continuous dialysis for measurement of endocytosis. *Exp. Parasitol.* **49**, 366-380.

Field, H., Farjah, M., Pal, A., Gull, K. and Field, M. C. (1998). Complexity of trypanosomatid endocytosis pathways revealed by Rab4 and Rab5 isoforms in *Trypansoma brucei*. *J. Biol. Chem.* **48**, 32102-32110.

Fivaz, M., Vilbois, F., Thurnheer, S., Pasquali, C., Abrami, L., Bickel, P. E., Parton, R. G. and van der Goot, F. G. (2002). Differential sorting and fate of endocytosed GPI-anchored proteins. *EMBO J.* **15**, 3989-4000.

Frevert, U. and Reinwald, E. (1988). Endocytosis and intracellular occurrence of the variant surface glycoprotein in *Trypansoma congolense*. *J. Ultrastruct. Mol. Struct. Res.* **99**, 137-149.

Futter, C. E., Gibson, A., Allchin, E. H., Maxwell, S., Ruddock, L. J., Odorizzi, G., Domingo, D., Trownbridge, I. S. and Hopkins, C. R. (1998). In polarized MDCK cells basolateral vesicles arise from clathrin-γ-adaptin-coated domains on endosomal tubules. *J. Cell Biol.* **141**, 611-623.

Gaidorov, I., Santini, F., Warren, R. A. and Keen, J. H. (1999). Spatial control of coated-pit dynamics in living cells. *Nat. Cell Biol.* **1**, 1-7.

Ghosh, R. N., Gelman, D. L. and Maxfield, F. R. (1994). Quantification of low density lipoprotein and transferrin endocytic sorting in HEp2 cells using confocal microscopy. *J. Cell Sci.* **107**, 2177-2189.

Griffiths, G., Black, R. and Marsh, M. (1989). A quantitative analysis of the endocytic pathway in baby hamster kidney cells. *J. Cell Biol.* **109**, 2703-2720.

Gruenberg, J. (2001). The endocytic pathway: a mosaic of domains. *Nat. Rev. Mol. Cell. Biol.* **2**, 721–729.

Grünfelder, C. G., Engstler, M., Weise, F., Schwarz, H., Stierhof, Y.-D., Boshart, M. and Overath, P. (2002). Accumulation of a GPI-anchored protein at the cell surface requires sorting at multiple intracellular levels. *Traffic* **3**, 547-559.

Grünfelder, C. G., Engstler, M., Weise, F., Schwarz, H., Stierhof, Y.-D., Morgan, G. W., Field, M. C. and Overath, P. (2003). Endocytosis of a

glycosylphosphatidylinositol-anchored protein via clathrin-coated vesicles, sorting by default in endosomes and exocytosis via RAB11-positive carriers. *Mol. Biol. Cell.* **14**, 2029-2040.

Haylett, T. and Thilo, L. (1986). Limited and selective transfer of plasma membrane glycoproteins to membrane of secondary lysosomes. *J. Cell Biol.* **103**, 1249-1256.

Jeffries, T. R., Morgan, G. W. and Field, M. C. (2001). A developmentally regulated Rab11 homologue in *Trypanosoma brucei* involved in recycling processes. *J. Cell Sci.* **114**, 2617-2626.

Landfear, S. M. and Ignatushchenko, M. (2001). The flagellum and flagellar pocket of trypanosomatids. *Mol. Biochem. Parasitol.* **115**, 1-17.

Langreth, S. G. and Balber, A. E. (1975). Protein uptake and digestion in bloodstream and culture forms of *Trypanosoma brucei. J. Protozool.* **22**, 40-53.

Mellmann, I. (1996). Endocytosis and molecular sorting. *Annu. Rev. Cell Dev. Biol*. **12**, 575–625.

Morgan, G. W., Allen, C. L., Jeffries, T. R., Hollingshead, M. and Field, M. C. (2001). Developmental and morphological regulation of clathrin-mediated endocytosis in *Trypanosoma brucei*. *J. Cell Sci.* **114**, 2605-2615.

Morgan, G. W., Hall, B. S., Denny, P. W., Carrington, M. and Field, M. C. (2002a). The kinetoplastida endocytic apparatus. Part I: a dynamic system for nutrition and evasion of host defences. *Trends Parasitol.* **18**, 491-496.

Morgan, G. W., Hall, B. S., Denny, P. W., Field, M. C. and Carrington, M. (2002b). The endocytic apparatus of the kinetoplastida. Part II: machinery and components of the system. *Trends Parasitol.* **18**, 540-546.

Mukherjee, S., Ghosh, R. N. and Maxfield, F. R. (1997). Endocytosis. *Physiol. Rev.* **77**, 759-803.

Nichols, B. J., Kenworthy, A. K., Polishchuk, R. S., Lodge, R., Roberts, T. H., Hirschberg, K., Phair, R. D. and Lippincott-Schwartz, J. (2001). Rapid cycling of lipid raft markers between the cell surface and Golgi complex. *J. Cell Biol.* **153**, 529-541.

O'Beirne, C., Lowry, C. M. and Voorheis, H. P. (1998). Both IgM and IgG anti-VSG antibodies initiate a cycle of aggregation-disaggregation of bloodstream forms of *Trypanosoma brucei* without damage to the parasite. *Mol. Biochem. Parasitol.* **91**, 165-193.

Overath, P., Stierhof, Y.-D. and Wiese, M. (1997). Endocytosis and secretion in trypanosomatid parasites – tumultuous traffic in a pocket. *Trends Cell Biol.* **7**, 27–33.

Pal, A., Hall, B. S., Nethbeth, D. N., Field, H. I. and Field, M. C. (2002). Differential endocytic functions of *Trypansoma brucei* Rab5 isoforms reveal a glycosylphospatidylinositol-specific endosomal pathway. *J. Biol. Chem.* **277**, 9529-9539.

Russo, D. C. W., Grab, D. J., Lonsdale-Eccles, J. D., Shaw, M. K. and Williams, D. J. L. (1993). Directional movement of variable surface glycoprotein-antibody complexes in *Trypanosoma brucei*. *Eur. J. Cell Biol.* **62**, 432-441.

Sabharanjak, S., Sharma, P., Parton, R. G. and Mayor, S. (2002). GPI-anchored proteins are delivered to recycling endosomes via a distinct cdc42-regulated, clathrin-independent pinocytic pathway. *Dev. Cell* **2**, 411-423.

Seyfang, A., Mecke, D. and Duszenko, M. (1990). Degradation, recycling, and shedding of *Trypanosoma brucei* variant surface glycoprotein. *J. Protozool.* **37**, 546–552.

Sharma, P., Sabharanjak, S. and Mayor, S. (2002). Endocytosis of lipid rafts: an identity crisis. *Cell Devel. Biol.* **13**, 205-214.

Skretting, G., Torgersen, M. L., van Deurs, B. and Sandvig, K. (1999). Endocytic mechanisms responsible for uptake of GPI-linked diphtheria toxin receptor. *J. Cell Sci.* **122**, 3899-3909.

Sönnichsen, B., de Renzis, S., Nielsen, E., Rietdorf, J. and Zerial, M. (2000). Distinct membrane domains on endosomes in the recycling pathway visualized by multicolour imaging of Rab4, Rab5 and Rab11. *J. Cell Biol.* **149**, 901-913.

Steinman, R. M., Brodie, S. E. and Cohn, Z. A. (1976). Membrane flow during pinocytosis. *J. Cell Biol.* **68**, 665-687.

Stoorvogel, W., Oorschot, V. and Geuze, H. J. (1996). A novel class of clathrin-coated vesicles budding from endosomes. *J. Cell Biol*. **132**, 21-33.

Thilo, L. (1985). Quantification of endocytosis-derived membrane traffic. *Biochim. Biophys. Acta* **822**, 243-266.

Thilo, L., Stroud, E. and Haylett, T. (1995). Maturation of early endosomes and vesicular traffic to lysosomes in relation to membrane recycling. *J. Cell Sci.* **108**, 1791-1803.

Webster, P. (1989). Endocytosis by African trypanosomes. I. Three-dimensional structure of the endocytic organelles in *Trypansoma brucei* and *T. congolense*. *Eur. J. Cell Biol.* **49**, 295-302.

Webster, P. and Grab, D. J. (1988). Intracellular colocalization of variant surface glycoprotein and transferrin-gold in *Trypansoma brucei. J. Cell Biol.* **106**, 279-288.

Webster, P. and Russell, D. G. (1993). The flagellar pocket of trypanosomatids. *Parasitol. Today* **9**, 201-206.